Effects of bias in solar radiative transfer codes on global climate model simulations

Albert Arking
Department of Earth and Planetary Sciences, Johns Hopkins University, Baltimore, Maryland, USA

Received 8 June 2005; revised 10 August 2005; accepted 9 September 2005; published 27 October 2005.

[1] Codes commonly used in climate and weather prediction models for calculating the transfer of solar radiation in the atmosphere show systematic differences amongst each other, and even the best of codes show systematic differences with respect to observations. A 1-dimensional radiative-convective equilibrium model is used to show the effects of such bias on the global energy balance and on the global response to a doubling of CO_2. We find the main impact is in the energy exchange terms between the surface and atmosphere and in the convective transport in the lower troposphere, where it exceeds 10 W m^{-2}. The impact on model response to doubling of CO_2, on the other hand, is quite small and in most cases negligible. **Citation:** Arking, A. (2005), Effects of bias in solar radiative transfer codes on global climate model simulations, *Geophys. Res. Lett.*, *32*, L20717, doi:10.1029/2005GL023644.

1. Introduction

[2] The accuracy of the radiation codes used in general circulation models for calculating the absorption of solar radiation in the atmosphere is still subject to question. For climate studies, what is important is not the error in calculating the radiative fluxes under a given set of conditions, but the systematic error that could occur over extended time and spatial scales. Systematic as well as random differences amongst codes of varying levels of detail have been revealed in organized intercomparisons, where radiative fluxes are compared for specified atmospheric conditions. Over the past 15 years, there has been little progress in reducing the differences [*Fouquart et al.*, 1991; *Barker et al.*, 2003; *Halthore et al.*, 2005].

[3] Of concern in this study are systematic differences, not only amongst the codes but what appears to be a general bias between the best of codes and observations. The principal bias is in the partitioning of absorbed solar radiation between the atmosphere and surface. We first look at examples of bias amongst several reanalysis data sets and between stand alone radiation codes and observations. Then we use a 1-dimensional radiative-convective equilibrium model (RCEM) to assess the potential impact on the global energy budget and on the global response to a doubling of CO_2.

2. Reanalyses Comparison

[4] Five-year global means of atmospheric and surface absorption are shown in Table 1 for three reanalyses: Goddard Earth Observing System-1 (GEOS-1), National Center for Environmental Prediction/National Center for Atmospheric Research Reanalysis (NCEP/NCAR), and the European Center for Medium-range Weather Forecasting (ECMWF) Re-Analysis (ERA-15). Although absorption is a characteristic of the model, and not the observational data assimilated into the model, total absorption compares well with measurements at the top of the atmosphere (TOA) over the same five-year period, based on the Earth Radiation Budget Experiment (ERBE), [*Barkstrom et al.*, 1989]. (The anomaly in NCEP is attributed to an unrealistic surface albedo over land, its effect seen in Table 1.) However, there are large differences in the partitioning of the absorbed energy between surface and atmosphere, with ERA-15 showing 50% greater atmospheric absorption than GEOS-1. Figure 1 shows that the bias is consistent across a wide range of latitudes.

[5] Observations of atmospheric absorption are only available where there are surface measurements. A collection of such measurements known as the Global Energy Budget Archive (GEBA) [*Ohmura and Gilgen*, 1993] has been used along with ERBE satellite measurements of total absorption to determine the atmospheric component. The overall mean and standard deviation determined from monthly mean values at 114 GEBA sites over the period Mar 1985–Dec 1988 are compared in Table 2 with collocated values in the reanalyses. Although the GEBA/ERBE sites are widely distributed, they are mostly on or near large land masses at mid latitudes in the Northern Hemisphere. The comparison with the GEBA/ERBE observations shows large underestimates in GEOS-1 and NCEP, and an overestimate of smaller magnitude in ERA-15. The standard deviations also differ significantly amongst the models.

3. Model Description

[6] To determine the impact of model bias in calculating atmospheric absorption on the global energy budget and on model response to external forcing, we conducted numerical experiments with the RCEM, a 1-dimensional radiative-convective equilibrium model. The basic physics and functional characteristics of the model are the same as in models frequently used in this type of study [e.g., *Lindzen et al.*, 1982]. It differs only in the use of a more up-to-date radiation code and in the method of achieving an equilibrium solution. The RCEM uses the radiative transfer code of *Chou* [1992] and *Chou and Lee* [1996] for solar radiation, and *Chou et al.* [1991] for terrestrial infrared radiation. The input to the radiation codes includes vertical profiles of temperature, water vapor, and aerosol and cloud optical properties, and surface albedo and solar zenith angle.

0094-8276/05/2005GL023644$05.00

Table 1. Global Mean Absorption Relative to the Incident Solar Flux at TOA, Mar 1985–Feb 1990

		Absorption		
Data Set	Sfc Albedo	Total	Sfc	Atmos
ERBE		0.703		
GEOS-1	0.129	0.716	0.553	0.163
NCEP	0.217	0.662	0.474	0.188
ERA-15	0.155	0.704	0.457	0.247

[7] Calculations of atmospheric absorption with Chou's solar radiation code are compared in Figure 2 with the RRTM code [*Clough et al.*, 2005] and with observations on 13 cloud-free days at the Atmospheric Radiation Measurement (ARM) program's Southern Great Plains (SGP) site (manuscript in preparation; for preliminary results see *Arking* [1999]). Each point represents the fraction of the incident solar flux at TOA absorbed by the atmosphere over the course of a day, based on continuous measurements of broadband surface flux integrated over one-minute intervals and TOA reflected flux estimated from narrow-band satellite observations at half-hour intervals. The input to the radiation code includes total column water vapor measured from nearby radiosondes, and onsite measurements of ozone, aerosol optical depth, and surface albedo. The shapes of the moisture, ozone, and aerosol profiles are prescribed based on a mid-latitude climatology. The single scattering albedo was set at 0.95 consistent with monthly mean statistics at the site [*Delene and Ogren*, 2002].

[8] Although clouds can have a large effect on atmospheric absorption on a day-to-day basis, the average effect over extended spatial and temporal scales is small [*Arking*, 1996, 1999], so that one would not expect the inclusion of clouds to significantly impact the thrust of this investigation.

[9] The logarithmic fit of the calculations and observations to column water vapor (solid lines in Figure 2) suggests an additional water vapor-dependent absorption can be added to the radiation codes that would remove the bias with respect to the observations. For Chou's code, we added an optical thickness in each atmospheric layer, uniform within the 400–700 nm band, with the following form:

$$d\tau = (a + bqp/p_o)dp/g \quad (1)$$

where q is specific humidity, p is pressure, g is earth's gravity, and a and b are constants. The first term represents an added absorption that is independent of the variable gases in the atmosphere, while the second term represents a pressure-dependent addition to the water vapor absorption coefficient. The constants determined to give a best fit are a = 4.3e-5 cm^2 g^{-1} and b = 0.016 cm^2 g^{-1}. The two terms contribute approximately equally for a column water vapor amount of $\sim$3 g cm^{-2}. Figure 2 shows that adding this enhanced absorption to Chou's radiation code yields a fairly good fit to the observations, increasing mean daily absorption by $\sim$0.04 relative to the incident solar flux at TOA (equivalent to $\sim$14 W m^{-2} daily average). A smaller enhancement applied to RRTM would have the same effect. In what follows, 'enhanced code' refers to Chou's code with the added absorption.

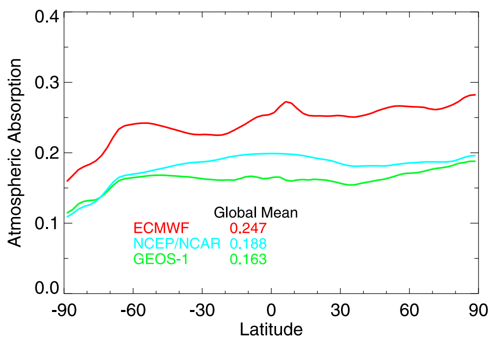

Figure 1. Mean atmospheric absorption of solar radiation in three reanalyses for the period March 1985–February 1990.

[10] The RCEM is based on a balance of energy at the surface and each level of the atmosphere, assuming only two types of energy transport: radiation and convection. Without convection, the lapse rate would increase with increasing pressure, at some point exceeding a specified lapse rate (e.g., dry or moist adiabatic, or a fixed lapse rate) beyond which the atmosphere would be considered unstable. We therefore assume that convection takes place, beginning at the surface and continuing upward to a point (defined as the tropopause) where the net radiative flux (solar plus terrestrial components) becomes zero. Below the tropopause, the temperature is constrained by the specified lapse rate, resulting in a calculated net upward radiative flux that is negative. Above the tropopause, the temperature is determined by requiring the net flux to be zero at all levels.

[11] Numerically, we achieve a solution by choosing a first guess for the tropopause pressure and a first guess temperature profile for each layer between the tropopause and TOA and the layer immediately below the tropopause. Air temperature in the layers below the top layer of the troposphere is constrained by the temperature of the top layer and the specified lapse rate. Surface temperature is made equal to the air temperature immediately above, based on the assumption that there are efficient energy exchange processes at the surface to eliminate any discontinuity. We then linearize the radiative transfer equation around the assumed set of temperatures, creating a matrix equation in which a vector of changes in flux at each level from the tropopause on up, is a matrix operator times the change in temperature in each layer from the top of the troposphere to TOA. Inversion of the operator by standard techniques yields a new set of temperatures, which is then used as the reference point for re-computing the matrix operator. This process is iterated until the magnitude of the net flux,

Table 2. Mean and Standard Deviation of the Ratio of Solar Energy Absorbed in the Atmosphere to Incident Solar Flux at TOA, Based on Monthly Mean GEBA/ERBE Observations and Collocated Grid Points in Three Reanalysis Data Sets, Mar 1985–Dec 1988

Data Set	Mean	Std Dev
GEBA/ERBE	0.242	0.048
GEOS-1	0.160	0.019
NCEP	0.190	0.010
ERA-15	0.277	0.031

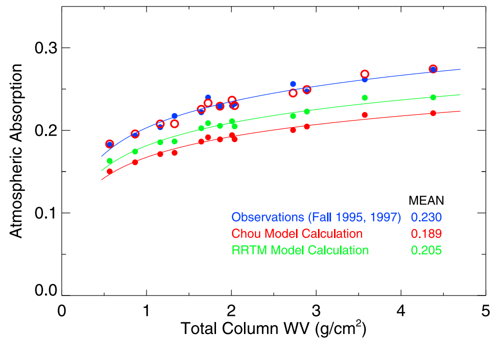

Figure 2. Mean daily absorption of solar radiation in the atmosphere on 13 clear days at the ARM/SGP site in Oklahoma, based on observations (blue) and two radiation models (green and red). Open circles are based on the Chou model with enhanced absorption according to Equation 1.

terrestrial plus solar, at the tropopause and at each level above is $\leq$0.01 W m^{-2}.

[12] The adjusted temperature, based on the assumed tropopause height, will not necessarily have a smooth transition between the tropopause and the layer above. To remove any substantial discontinuity, we iteratively adjust the tropopause height until we satisfy a specified smoothness criterion. The final solution is a complete temperature profile, with the net radiative flux computed at each level within the troposphere, where it is not zero. Due to the lapse rate constraint, the net upward flux below the troposphere is negative. Since convection is assumed to make up the deficit, the magnitude of the net flux is considered the convective flux, which is positive upward.

[13] The model allows a solution either for a specified incoming solar flux or to match a specified net flux at TOA. The model also has an option for a prescribed water vapor feedback. The present runs were made both with fixed specific humidity (i.e., no feedback) and fixed relative humidity, a feedback similar in performance to many 3-dimensional models. Although the model also allows clouds to be specified, we present results only for cloud-free conditions, since they illustrate the main point without the additional complication.

4. Results for Current CO_2 Level

[14] Equilibrium results showing the effects of enhanced absorption appear in Figure 3, with key variables from each run shown in Table 3. The incident solar flux at TOA is fixed at 342 W m^{-2} at a zenith angle of 60°, base CO_2 concentration is 360 ppm, surface pressure is 1013 hPa, and humidity (specific humidity for 'fixed q', relative humidity for 'fixed RH') corresponds to that of a mid latitude summer climatology. Figure 3 shows model results for fixed q, with either of two specified lapse rates: a moist adiabatic, and a fixed lapse rate of 6.8 K km-1 (0.7 times the dry adiabatic). The main effect of the lapse rate specification is on the distribution of temperature within the troposphere; in the moist adiabatic cases the boundary layer is cooler and the mid troposphere warmer. A more physically-based parameterization of cumulus convection yields results between the moist adiabatic and fixed lapse rates [*Lindzen et al.*, 1982].

[15] As seen in Table 3, enhanced absorption increases surface temperatures by less than 1 K in all cases. Within the troposphere (LHS of Figure 3), the increases are less than 1 K for fixed lapse rate, and less than 1.3 K for the moist adiabatic. This relatively small effect is a consequence of the enhanced absorption of solar radiation causing mostly a redistribution of the absorption between surface and atmosphere, with a relatively small impact on the net radiative flux at the tropopause ($\sim$1.5 W m^{-2}). In the stratosphere, where the net radiative effect (net flux at TOA minus that at the tropopause) is larger ($\sim$3 W m^{-2}, due primarily to the a term in Equation 1), the increase in temperature is correspondingly larger (3–6 K between 100 and 200 hPa). For the entire column, the planetary albedo decreases by 0.013, corresponding to a net forcing at TOA of $\sim$4.5 W m^{-2}.

[16] The impact of enhanced absorption on the convective flux at the surface is shown on the RHS of Figure 3. At the surface, the convective flux (Table 3, 5th column) is decreased in all cases by 15–17 W m^{-2}. The bulk of that change is due to a shift of absorbed solar energy from the surface to the atmosphere, in addition to a small increase in total column absorption. Three-dimensional model studies with Version 3 of the NCAR Climate Community Model shows that the latent heat effect reduction is $\sim$10% globally, implying a $\sim$10% reduction in global evaporation and precipitation (F. Liu, PhD dissertation, Johns Hopkins University, 2002).

5. Results for 2 $\times$ CO_2

[17] The effects of enhanced absorption on model response to a doubling of CO_2 are shown in Table 3, and plotted data are shown in Figure 4 for the fixed lapse rate cases, with (fixed RH) and without (fixed q) a prescribed water vapor feedback. The moist adiabatic cases have an additional feedback associated with the response of the lapse rate to changes in temperature, which is negative (unlike water vapor feedback, which is positive). As pointed out by *Lindzen et al.* [1982], the moist adiabat forces the response to occur at a higher level in the troposphere, allowing a more efficient terrestrial emission to space. Note

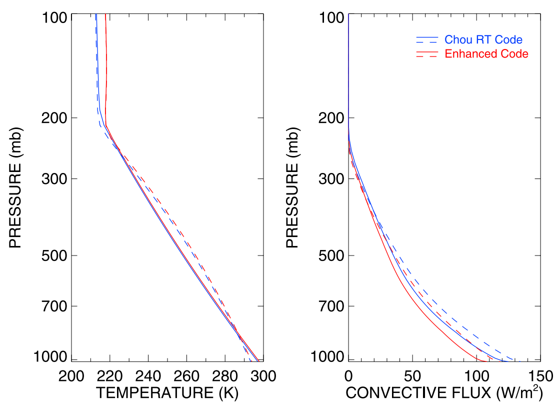

Figure 3. Equilibrium temperature (LHS) and convective flux (RHS) profiles from a 1-d radiative-convective model with fixed lapse rate (solid lines) and moist adiabatic lapse rate (dashed lines), showing the effects of enhanced absorption (red) added to Chou's radiation code (blue).

Table 3. Key Variables of RCEM Runs[a]

Code	P_{TR}	CWV	T_S	$CONV_S$	ALB	ABS	NET_{TR}	NET_{TOA}	ΔF
				1 × CO_2					
C-qd	200	2.73	297.06	124.98	0.141	0.222	279.29	293.87	4.85
E-qd	220	2.73	297.85	108.28	0.128	0.278	280.21	298.07	4.92
C-qm	220	2.73	293.39	134.62	0.141	0.222	278.67	293.87	4.90
E-qm	220	2.73	293.94	118.58	0.128	0.278	280.22	298.07	5.03
C-rd	220	2.18	294.30	124.47	0.142	0.214	278.69	293.51	4.88
E-sd	240	2.18	295.00	109.02	0.130	0.267	279.19	297.47	4.95
C-rm	240	2.57	292.87	131.14	0.141	0.219	278.40	293.75	4.87
E-sm	240	2.57	293.38	115.58	0.129	0.274	279.62	297.88	5.01
				2 × CO_2 − 1 × CO_2					
C-qd	0	0.00	1.15	−1.78	0.000	0.000	0.01	0.00	−0.03
E-qd	0	0.00	1.16	−1.80	0.000	0.000	0.00	0.00	−0.02
C-qm	0	0.00	0.83	−1.01	0.000	0.000	0.00	0.00	−0.01
E-qm	0	0.00	0.83	−1.03	0.000	0.000	−0.01	0.00	−0.01
C-rd	0	0.31	2.00	3.75	−0.001	0.005	0.21	0.23	0.01
E-sd	−20	0.31	2.06	2.93	−0.001	0.008	1.16	0.37	0.09
C-rm	−20	0.37	1.65	3.84	−0.001	0.005	0.67	0.24	−0.06
E-sm	−20	0.37	1.70	2.96	−0.001	0.008	1.10	0.41	−0.07

[a]Code: 1st character indicates RT code (C = Chou, E = enhanced); 2nd character indicates water vapor specification: fixed specific humidity (q) or fixed RH (r) corresponding to a mid latitude summer climatology, or specified specific humidity corresponding to that in previous run; 3rd character indicates lapse rate specification: 0.7 × dry adiabatic (d) which is 6.8 K km^{-1}, or moist adiabatic (m). P_{TR}: Pressure at tropopause (top of convection zone). CWV: column water vapor (g cm^{-2}). T_S: surface temperature (K). $CONV_S$: convective flux at surface (i.e., sensible plus latent heat exchange). ALB: planetary albedo at TOA. ABS: solar flux absorbed in atmosphere. NET_{TR}, NET_{TOA}: net solar flux (equal to net terrestrial flux) at tropopause and TOA, respectively. ΔF: longwave radiative forcing at tropopause due to doubling of CO_2.

that whenever RH is fixed for the run with the standard radiation code, the RH for the run with the enhanced code is specified (denoted by an 's' in column 1 of Table 3) to be the same as that obtained for the corresponding standard run.

[18] These results show that the effect of enhanced absorption on the tropospheric temperature response to a doubling of CO_2 is negligible for all cases. The effect on the convective flux is appreciable only in the presence of water vapor feedback; with our feedback (fixed RH) the convective flux is reduced by ~1 W m^{-2}.

6. Discussion and Conclusion

[19] The radiative properties of the clear atmosphere are such that about half the solar radiation incident at TOA is absorbed by the surface, and only ~25% is absorbed by the atmosphere. Hence, it is the surface that is the primary source of heat for the troposphere, most of which is in the form of emitted (infrared) radiation, but some of it is in the form of a thermodynamic heat exchange at the surface (comprising sensible and latent heat) that is carried upward by convection. Enhancing atmospheric absorption of solar radiation would transfer to the atmosphere some of the solar energy that would otherwise heat the surface.

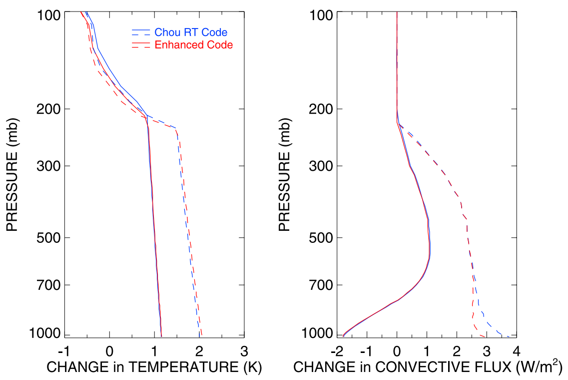

Figure 4. The response of the RCEM to a doubling of CO_2. with (dashed lines) and without (solid lines) water vapor feedback, showing the effects of enhanced absorption (red) added to Chou's radiation code (blue).

[20] As one might expect from a change in the radiation code which increases the absorption of solar radiation in the atmosphere, energy that is otherwise primarily absorbed by the surface is captured by the atmosphere. Hence, as we see in Figure 3, the convective flux necessarily decreases. The magnitude of the change seen, 15–17 W m^{-2} at the surface, probably exaggerates the effect because the simulations were done under clear sky conditions. There is also a small increase in tropospheric temperatures, related to a small increase in column absorption below the tropopause, and a larger increase in stratospheric temperatures due to the increase of absorption above the tropopause.

[21] In examining the response of the atmosphere to a doubling of CO_2, we find the effects of enhanced absorption are much smaller because we are now looking at differences of differences. The effect on the tropospheric temperature is negligible, and the effect on the convective flux response is non-negligible only near the surface when we allow water vapor feedback.

[22] **Acknowledgment.** The author acknowledges Ming-Dah Chou for helpful discussions and for providing his solar and infrared radiation codes, Jean-Jacques Morcrette and Siegfried Schubert for providing the data sets and explanations relating to the ECMWF ERA-15 and GEOS-1 reanalyses, respectively, and Eli Mlawer for providing the RRTM radiation code.

References

Arking, A. (1996), Absorption of solar energy in the atmosphere: Discrepancy between model and observations, *Science*, *273*, 779–782.

Arking, A. (1999), The influence of clouds and water vapor on atmospheric absorption, *Geophys. Res. Lett.*, *26*, 2729–2732.

Barker, H. W., et al. (2003), Assessing 1D atmospheric solar radiative transfer models: Interpretation and handling of unresolved clouds, *J. Clim.*, *16*, 2676–2699.
Barkstrom, B., et al. (1989), Earth radiation budget experiment (ERBE) archival and April 1985 results, *Bull. Am. Meteorol. Soc.*, *70*, 1254–1262.
Chou, M.-D. (1992), A solar radiation model for use in climate studies, *J. Atmos. Sci.*, *49*, 762–772.
Chou, M. D., and K. T. Lee (1996), Parameterizations for the absorption of solar radiation by water vapor and ozone, *J. Atmos. Sci.*, *53*, 1203–1208.
Chou, M.-D., D. P. Kratz, and W. L. Ridgway (1991), Infrared radiation parameterizations in numerical climate models, *J. Clim.*, *4*, 424–437.
Clough, S. A., et al. (2005), Atmospheric radiative transfer modeling: A summary of the AER codes, *J. Quant. Spectrosc. Radiat. Transfer*, *91*, 233–244.
Delene, D. J., and J. A. Ogren (2002), Variability of aerosol optical properties at four North American surface monitoring sites, *J. Atmos. Sci.*, *59*, 1135–1150.
Fouquart, Y., B. Bonnel, and V. Ramaswamy (1991), Intercomparing shortwave radiation codes for climate studies, *J. Geophys. Res.*, *96*, 8955–8968.
Halthore, R. N., et al. (2005), Intercomparison of shortwave radiative transfer codes and measurements, *J. Geophys. Res.*, *110*, D11206, doi:10.1029/2004JD005293.
Lindzen, R. S., A. Y. Hou, and B. F. Farrell (1982), The role of convective model choice in calculating the climate impact of doubling CO_2, *J. Atmos. Sci.*, *39*, 1189–1205.
Ohmura, A., and H. Gilgen (1993), Re-evaluation of the global energy balance, in *Interactions Between Global Climate Subsystems: The Legacy of Hann*, *Geophys. Monogr. Ser.*, vol. 75, edited by G. McBean and M. Hantel, pp. 93–110, AGU, Washington, D. C.

A. Arking, Department of Earth and Planetary Sciences, Johns Hopkins University, Baltimore, MD 21218, USA. (arking@jhu.edu)